Subjective and objective speech intelligibility investigations in primary school classrooms

A time-independent reliability based design approach for rockfall net fences: a comparative analysis within the Eurocode framework

IOP Conf. Series: Earth and Environmental Science **833** (2021) 012189 doi:10.1088/1755-1315/833/1/012189

A time-independent reliability based design approach for rockfall net fences: a comparative analysis within the Eurocode framework

Maddalena Marchelli, Daniele Peila
DIATI, Politecnico di Torino, Torino, Italy
E-mail: maddalena.marchelli@polito.it

Valerio De Biagi
DISEG, Politecnico di Torino, Torino, Italy

Abstract. The design of net fences as passive mitigation measures against rockfall events has represented a challenge since the last decades. The choice of the proper effect of the actions to consider in the design is still under debate. Recently, the Authors have proposed a novel time-independent reliability approach encompassing the large variability of the size and the kinematics of the possible impacting blocks. The entire statistics of all these quantities (size, velocity, and height) enters into the calculations, differently from other approaches that consider specific values of the parameters. In addition, the variability in time of the inputs is tackled, with particular reference to the size of the falling block. The recent approach is herein merged and compared with the current semi-probabilistic ultimate limit state design approach, suggested in the Eurocodes and implemented in the Italian recommendations UNI 11211-4:2018, with the purpose of finding the equivalent partial safety factors of kinetic energy and trajectory height of the impacting block. A sensitivity analysis with different synthetic profiles, representing possible real situations, is performed highlighting that if a set of partial safety factors is assigned to different sites, an intrinsic variability in the failure probability has to be accepted.

1. Introduction

Rockfall represents one of the major hazards in mountain environment [1, 2] where the implementation of effective structural mitigation measures is often required [3, 4, 5]. Installing net fences is a possible solution for risk management. Different solutions to realize these systems, defined as construction protection kits, have been proposed, improving the adopted components, material, and the assembly [4, 6, 7]. As a consequence, the efficient design of these structural measures has been of particular interest, even though a codified design solution has not been defined yet. UNI 11211-4 [8] in Italy and ONR 24810 [9] in Austria constitute the existing national standards, only.

The prescriptive-based design for each component, according to which standards on material, configuration, strength and stiffness have to be guaranteed, is not feasible for complex and unique structural systems [10]. On the contrary, the performance-based design [11] has been often adopted for assembled structures, allowing more comprehensible design requirements, and,

thus, the quality and innovation of the systems. This design approach is based on the premise that structural systems have to achieve specific performance objectives and, thus, the definition of the end goal is the starting point of the design process. A hybrid solution is adopted for net fences. The producers identify optimal new technologies and solutions and assess the complying performance through numerical analyses [12, 13, 14, 15, 6, 16, 17, 18] and testings, according the requests of EAD 340059-00-0106 [19]. In details, the performance is related to the interception and stopping of falling blocks with a height and kinetic energy. Once installed on a slope, due to the variability of the conditions and the random nature of the phenomenon, the barrier can experience a multitude of impacts different from the ones for which the kits were tested. Hence, prescriptive-based approaches are thus necessary to guarantee an adequate level of safety, which is measured through the reliability of the system. The reliability-based design consists in a procedure which allows considering the random nature of the parameters describing a structure and the actions on it [20]. In the framework of the ultimate limit state design suggested by EC7 [21], the following inequalities must be verified:

$$h_{B,d} \geq h_{b,d} + t \qquad \text{and} \qquad E_{B,d} \geq \frac{1}{2} m_d v_d^2, \tag{1}$$

where $h_{B,d}$ and $E_{B,d}$ are the height and the energy absorption capacity of the system, respectively, and $h_{b,d}$, m_d, v_d the height, velocity, and mass of the impacting block. Subscript $_d$ stands for design value. The term t, i.e. the tolerance, serves for considering that the height is generally computed in the center of mass of the block. To compute each term, partial safety factors are applied accounting for the variability of the effects of the actions and the resistances. These factors are applied to the reference, say characteristic (subscript $_k$), value of each parameter, selected among the probabilistic distribution describing the parameter itself. UNI 11211-4 [8] and ONR 24810 [9] provide the factors for computing the design values of the variables. While UNI 11211-4 considers fixed factors, ONR 24810 differentiates the factors according to the expected frequency of the events and the importance class of the protected elements at risk.

In civil structural framework, the partial safety factors are computed starting from a given value of the reliability index β, i.e. a measure of the safety. To differentiate the failure probability of rockfall protection structures, a novel time-independent reliability approach (TIRA) has been recently proposed by the Authors [7, 22, 23], encompassing the large variability of the size and the kinematics of the possible impacting blocks.

The present research work aims at comparing the results of the full reliability calculations (TIRA) with those obtained with fixed partial safety factors (PSFA) in terms of design energy and height of the barrier and failure probabilities. Aiming at representing all the most frequent rockfall hazardous situations, different synthetic profiles were adopted for performing 2D trajectory analyses. Section 2 deals with with the basis of the proposed method, while the performed trajectory analyses and the consequent design of the net fence according to both PSFA and TIRA are outlined in Section 3. Results and discussions are presented in Section 4, while in Section 5 conclusions and future perspective are defined.

2. Failure mechanisms and reliability-based design approach

This section provides the pivotal principles of the reliability approach for rockfall protection structures proposed in [22, 23] and enhanced in [24]. Herein, the theory behind the approach is briefly described. Considering that the required performances are related to the interception and the stop of an impacting block, the possible failure modes can be simplified into a failure mode connected to the exceeding height when the block is not intercepted, and one connected to the exceeding kinetic energy when the energy absorption capacity is smaller than block translational energy. A failure probability is associated to each mode, F_h and F_e, respectively.

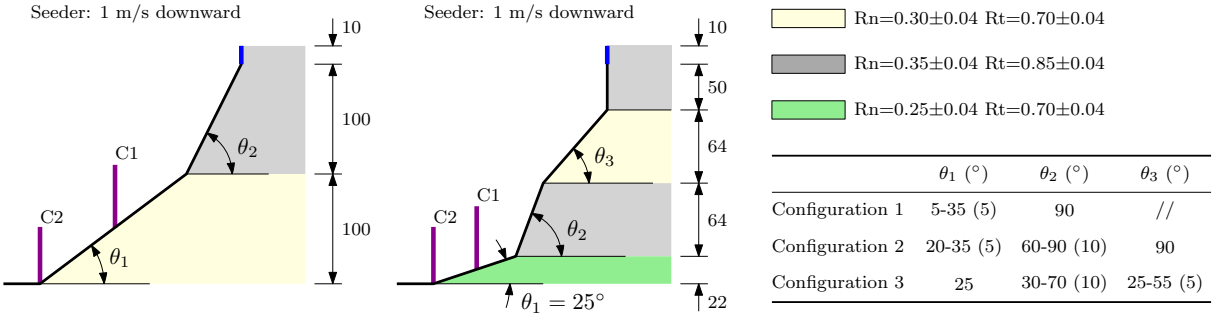

	θ_1 (°)	θ_2 (°)	θ_3 (°)
Configuration 1	5-35 (5)	90	//
Configuration 2	20-35 (5)	60-90 (10)	90
Configuration 3	25	30-70 (10)	25-55 (5)

Figure 1. Sketch of the synthetic slope profiles adopted for the simulations (measures are in meters), coefficients of restitution and slope angles (in brackets the interval step is reported). The blue line represents the linear seeder.

Each failure mode outlines a scenario mathematically described through a limit function, i.e. the boundary between failure and safety, derived from a state function. Under lumped-mass assumption, for a given point along the slope where the net fence would be installed, independent probability distributions of velocity and height can be computed [25, 26, 27, 28]. Referring to falling block masses, following [29], for a given return period T a distribution of values centered in $m_{50}(T) = M_{th}(\lambda T)^{1/\alpha}$, where α is the shape coefficient of a Pareto Type I distribution accounting for the heterogeneity of the size of the possible impacting blocks, M_{th} is the threshold mass, i.e. the minimum mass of an impacting block whose occurrence frequency is λ, can be defined.

Considering the resistances, the energy absorption capacity and height are generally evaluated according to the assessment procedure of EAD 340059-00-0106 [19] and, as no information exists related to their variability [30], as a simplification, these quantities can be assumed having a Dirac-δ distribution on the CE certified absorption capacity and nominal height, respectively. The reliability calculations are integrated over time (time-independent), in such a way that all the possible scenarios coupled with their occurrence probability are simulated. Following the procedure illustrated for the height in [24] and for the energy in [22], the failure probabilities in a given time of period τ (generally one year or the expected working life of the barrier) can be computed. Viceversa, knowing the failure probability, the design values of the variables can be determined.

3. Methods

To compare TIRA and PSFA approaches, with a commonly used procedure [31, 32, 33] synthetic slopes profiles were used to represent the most common real situations [34]. The basic idea is that the volume and the topography are the parameters that mostly affects the results [35, 36, 37, 38, 39, 40]. Thus, the influence of the variability of the topography was investigated Three configurations were considered (Fig. 1), varying slope angles. For each profile, trajectory analyses under lumped-mass assumption were carried out. Normally distributed restitution coefficients (R_n and R_t) were considered to account for the variability of block-slope interaction phenomena, representing typical real situations [41, 42]. A 10 m long vertical line seeder above the upper part was used as source location for all the simulated rock falls (10000 released blocks with a Monte Carlo sampling technique around the distributions of the restitution coefficients). A uniform distribution along the length of the seeder was used for the released point. Two collectors ($C1$ and $C2$) were positioned in the vertical direction at the middle and the end of the slope toe.

It is worth underlining that in the PSFA the choice of the mass represents a crucial aspect,

while in the TIRA for a given site, the calculations are performed on all the possible masses, considering their occurrence frequency. The results of the trajectory analyses, in terms of height and velocity distributions, served as input parameters for both TIRA and PSFA. In the former, as reported in [22, 23, 7], the 95th and the 99th percentiles were used to define a normal distribution for both height and velocity, later adopted into the calculations. On the contrary, in the PSFA the characteristic values (95th percentile) are used [8], only. According to UNI 11211-4 [8], the choice of the characteristic value of the mass m_k is remitted to the designer with the condition that it has to be assumed equal or greater than the 95th percentile of the distribution of the possible masses, neglecting the temporal aspect. In the following, m_k was derived as the 95th percentile of the distribution of the blocks at the foot of the cliff.

Firstly, for the PSFA, height and energy design values (namely $\tilde{h}_{B,d}$ and $\tilde{E}_{B,d}$) were computed applying the procedure suggested by UNI 11211-4 [8], with $\tilde{\gamma}_{h_b}$ equal to 1.21 and $\tilde{\gamma}_E$ equal to 1.93 (representing the most cautelative conditions), as $\tilde{h}_{B,d} = h_{95}\tilde{\gamma}_{h_b} + \left(\frac{3m_k}{4\pi\rho}\right)^{1/3}$ and $\tilde{E}_{B,d} = \frac{1}{2}m_k v_{95}^2\tilde{\gamma}_E$. The failure probability $\tilde{p}_f$ associated to $\tilde{h}_{B,d}$ and $\tilde{E}_{B,d}$ was computed according to the TIRA procedure. Secondly, given a failure probability p_f equal to 10^{-3}, considered as a feasible threshold for tolerable risk, the TIRA procedure was used to compute the correspondent $h_{B,d}$ and $E_{B,d}$.

4. Results and discussion

Table 1 reports the results obtained from the trajectory analyses performed with RocFall software [43]. Only the configurations for which the collectors were impacted are herein reported. A variety of results can be observed, in terms of both characteristic values and distribution trends, evaluated approximately through the ratio between the 99th and 95th values, ranging from 1 to a maximum of 2.33 and 9.13, for the velocity and the height respectively. Table 2 reports in columns 2 and 3, 7 and 8 the design values of height and energy according to the PSFA. The resulting failure probability $\tilde{p}_f$, computed through the TIRA procedure is reported in columns 4 and 9 for Collectors $C1$ and $C2$, respectively. Columns 5 and 6, 10 and 11 report the design values of height and energy given a failure probability 1×10^{-3}.

Applying the PSFA and considering the different configurations and collector positions, the results highlight that the correspondent $\tilde{p}_f$ assumes values differing for each situation, spanning from 2×10^{-3} to 10^{-1}, with a median of 1.3×10^{-2} for $C1$ and from 7×10^{-3} to 3×10^{-2}, with a median value of 10^{-2} for $C2$. Even if not directly reported, both failure modes affect the global failure in a similar manner. A previous paper [23] highlighted the influence of the inputs on the correspondent failure probability.

Performing the calculations with TIRA for a p_f equal to 10^{-3}, the values of both $h_{B,d}$ and $E_{B,d}$ are greater than the one evaluated with PSFA. Figure 2 displays the results in terms of γ_E, γ_{h_b}, resulting from:

$$\gamma_E = \frac{E_{B,d}}{1/2 m_{95} v_{95}^2} \qquad \text{and} \qquad \gamma_{h_b} = \frac{h_{B,d} - \left(\frac{3}{4\pi\rho}m_k\right)^{1/3}}{h_{95}}. \tag{2}$$

It is worth reminding that in a previous paper [24], the Authors suggested to consider a partial safety factor for the height including the shape of the block (γ_H), similarly to what reported in ONR 24810 [9], while UNI 11211-4 [8] considers a partial safety factor γ_{h_b} only applied to h_{95}. This partial safety factor was evaluated as:

$$\gamma_H = h_{B,d_R}\left[h_{95} + \left(\frac{3}{4\pi\rho}m_k\right)^{1/3}\right]^{-1}. \tag{3}$$

Table 1. Results of the performed 2D trajectory analyses on the proposed synthetic profiles for collectors $C1$ and $C2$.

$\theta_1, \theta_2, \theta_3$	Collector $C1$				Collector $C2$			
	v_{95} (m/s)	v_{99} (m/s)	h_{95} (m)	h_{99} (m)	v_{95} (m/s)	v_{99} (m/s)	h_{95} (m)	h_{99} (m)
25-90	2.54	2.55	0.01	0.01	10.20	11.34	0.01	0.01
30-90	9.30	10.63	0.01	0.01	17.20	17.82	0.01	0.01
35-90	14.42	21.11	0.07	1.23	10.44	11.39	0.01	0.01
20-80	0.79	0.79	0.01	0.01	10.11	11.22	0.01	0.01
20-90	2.98	2.99	0.01	0.01	10.03	10.99	0.01	0.01
25-60	7.35	8.70	0.01	0.01	9.62	10.70	0.01	0.01
25-70	7.51	9.31	0.01	0.01	15.75	16.25	0.01	0.01
25-80	9.61	17.54	0.06	0.55	15.54	16.32	0.01	0.01
25-90	14.27	17.67	0.43	2.18	14.81	15.52	0.01	0.01
30-60	11.28	12.31	0.01	0.01	14.47	22.31	0.09	0.60
30-70	15.39	20.44	0.04	0.71	3.73	4.40	0.01	0.01
30-80	18.62	31.01	1.07	1.72	4.18	5.03	0.01	0.01
30-90	29.03	31.01	2.43	10.84	3.78	4.22	0.1	0.1
35-60	13.61	14.48	0.01	0.01	4.45	5.10	0.1	0.1
35-70	21.10	31.00	0.62	1.01	4.01	4.87	0.1	0.1
35-80	30.44	31.01	5.23	9.38	7.17	8.71	0.1	0.1
35-90	30.67	30.67	14.47	19	5.75	13.40	0.1	0.1
25-40-45	6.66	7.47	0.09	0.09	7.46	13.40	0.14	0.31
25-40-55	7.59	8.69	0.09	0.09				
25-50-45	7.41	8.05	0.09	0.09				
25-50-55	8.05	8.82	0.09	0.09				
25-60-45	7.57	8.48	0.09	0.09				
25-60-55	15.26	20.01	0.23	1.35				
25-70-45	10.34	17.20	0.24	0.91				
25-70-55	16.53	17.55	5.05	6.05				

This suggestion originates observing that for h_{95} close to zero, i.e. sliding/rolling block, very high values of γ_{h_b} arise. In the boxplot, the median value is indicated by the central red line, while the bottom and the top edges indicate the 25th (Q_1) and 75th (Q_3) percentiles, respectively. The top of the upper whisker is located at $Q_3 + 1.5\,(Q_3 - Q_1)$. Larger values, namely, the outliers, are plotted as red crosses. Considering the γ_E values, the results show values inside $Q1$ and $Q3$ ranging from 5.1 to 7.4, with greater value, almost for the collector $C1$ (median value of 6.25 for $C1$ and 5.58 for $C2$). To better appreciate this aspect, a zoom on the values under the top of the upper whisker was reported inside the subfigure. Nevertheless, very high values can be observed, reported as red cross. As can be observed from the results reported in Table 2 and observed in [22], the greater the difference between v_{99} and v_{95}, the smaller the value of the correspondent partial safety factor γ_E, until $v_{99}/v_{95} \approx 1.5$, above which a trend reversal occurs. This observation is due to the fact that the uncertainty related to the mass decreases more rapidly than the increase uncertainty associated to the velocity.

Both γ_H and γ_{h_b} are influenced by h_{95} and h_{99}/h_{95}, even though the influence of the latter is more appreciable. Neglecting γ_{h_b}, for which values greater than 56 can be observed, for sliding block with $h_{99}/h_{95} = 1$, γ_H shows values inside $Q1$ and $Q3$ ranging from 1.4 to 1.8, with a median at 1.69 for $C1$, and from 1 to 1.7 for $C2$, with median at 1.45. Considering the whiskers, a range between 1 and 5.74 can be assumed as representative of the majority of the cases.

To better appreciate the compliance between the value of the partial safety factor and the

Table 2. Results of the performed analyses with PSFA and TIRA for collectors $C1$ and $C2$.

	Collector $C1$					Collector $C2$				
$\theta_1, \theta_2, \theta_3$	$\tilde{h}_{B,d}$ (m)	$\tilde{E}_{B,d}$ (kJ)	$\tilde{p}_f$ (-)	$h_{B,d}$ (m)	$E_{B,d}$ (kJ)	$\tilde{h}_{B,d}$ (m)	$\tilde{E}_{B,d}$ (kJ)	$\tilde{p}_f$ (-)	$h_{B,d}$ (m)	$E_{B,d}$ (kJ)
25-90	1.2	128	0.016	1.78	541	1.20	2067	0.010	1.78	5813
30-90	1.2	1719	0.009	1.78	4469	1.20	5878	0.014	1.78	21564
35-90	1.3	4132	0.016	3.32	13394	1.20	2166	0.011	1.78	6480
20-80	1.2	12	0.007	1.78	47	1.20	2031	0.010	1.78	5743
20-90	1.2	176	0.016	1.78	749	1.20	1999	0.011	1.78	5893
25-60	1.2	1073	0.009	1.78	2582	1.20	1839	0.010	1.78	5164
25-70	1.2	1121	0.008	1.78	2509	1.20	4929	0.014	1.78	18413
25-80	1.3	1835	0.037	2.17	35501	1.20	4798	0.013	1.78	16617
25-90	1.7	4046	0.017	4.89	9072	1.20	4358	0.013	1.78	15228
30-60	1.2	2528	0.011	1.78	7557	1.30	4160	0.014	2.22	23018
30-70	1.3	4706	0.011	2.38	9996	1.20	276	0.009	1.78	669
30-80	2.5	6889	0.020	3.38	72313	1.20	347	0.008	1.78	811
30-90	4.2	16745	0.027	20.96	54155	1.3	284	0.004	1.71	788
35-60	1.2	3681	0.012	1.78	12092	1.3	393	0.004	1.71	1016
35-70	2	8846	0.008	2.68	29867	1.3	320	0.002	1.71	736
35-80	7.5	18412	0.023	14.74	72807	1.30	1022	0.002	1.71	2351
35-90	18.7	18691	0.009	24.78	70700	1.30	657	0.102	1.71	43014
25-40-45	1.3	881	0.013	2.47	2413	1.40	1106	0.035	2.31	19395
25-40-55	1.3	1145	0.013	2.47	2964					
25-50-45	1.3	1091	0.015	2.47	3314					
25-50-55	1.3	1288	0.014	2.47	3797					
25-60-45	1.3	1139	0.013	2.47	3130					
25-60-55	1.5	4627	0.014	3.40	9882					
25-70-45	1.5	2124	0.022	2.58	22104					
25-70-55	7.3	5429	0.009	7.98	17985					

ratio between the 99th and the 95th percentiles, Figure 2 displays also the boxplots of v_{99}/v_{95} and h_{99}/h_{95}. Combining this representation with the value of Table 2, it appears how the shapes of the distributions of both velocity and height, simplified through v_{99}/v_{95} and h_{99}/h_{95} greatly affect the values of the correspondent partial safety factors.

Analyzing both γ_E and γ_H it seems that the choice of characteristic values equal to the 95th percentile of the distribution might not be sufficiently cautelative. As an example, for v_{99}/v_{95} greater than ≈ 1.5, if $v_k = v_{99}$, the equivalent γ_E displays a percentile reduction up to 250%. This reduction is not so appreciable for $v_{99}/v_{95} \approx 1$. Similar consideration can be performed for γ_H, especially for v_{99}/v_{95} greater than ≈ 2.

5. Conclusions

Net fences are one of the most adopted passive mitigation measures against rockfall. Different technologies have been developed, resulting in very complex systems assessed on the basis of [19]. In this framework, the assessment of the proper effect of the actions to consider as input parameter constitutes a key aspect, nowadays still under debate. Today's mandatory regulation does not treat specifically such systems, and only the Italian [8] and Austrian [9] standards address this topic, in the framework of a partial safety factor approach (PSFA), within the Eurocode framework. The proposed factors do not account neither for a given failure probability, nor for the site specificity of the problem and consider the size and the kinematics of the possible impacting blocks through point values (characteristic values). A recent work based on the

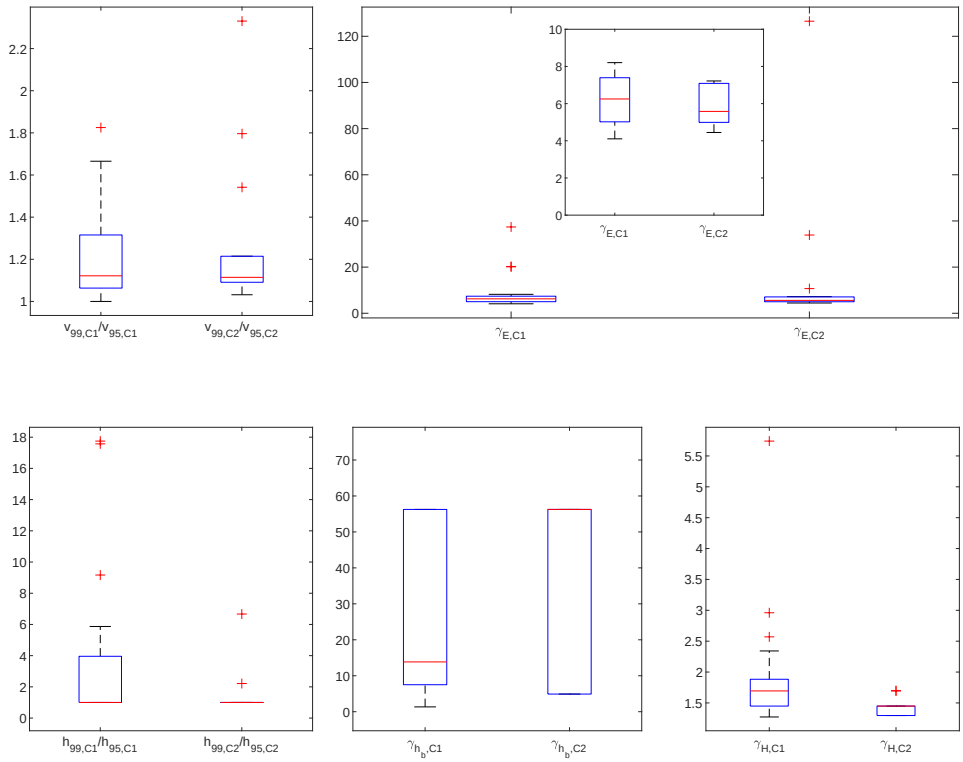

Figure 2. Boxplots of v_{99}/v_{95},h_{99}/h_{95}, γ_E, γ_H for both collector $C1$ and $C2$

time integration of the failure probability has shown interesting opportunities for the design of such structures, for a target failure probability. Given different synthetic profiles representing common scenarios, the true failure probabilities of net fences designed according to the PSFA were computed, revealing that, with fixed safety factors, a unique value of failure probability $\tilde{p}_f$ cannot be achieved. As a consequence, the TIRA was applied aiming at finding the equivalent partial safety factors for a given $p_f = 10^{-3}$. The obtained results highlights that the design value for the kinetic energy of the block can be several times its characteristic value (95th percentile) with large variability of the partial safety factors. A reduction of such variability was observed considering the 99th percentile of distribution as characteristic value.

To conclude, it results that if a set of partial safety factors is assigned to different sites, an intrinsic variability in the failure probability has to be accepted. Consequently, for a given failure probability, quantifying a unique set of partial safety factors valid for different sites cannot be achieved. A profitable solution for predisposing effective mitigation measures stands in the adoption of a reliability-based design approach with non-fixed factors. Further developments should be done in order to consider the influence of the site specificity for the evaluation of the mass and the assumption related to its characteristic value.

References

[1] Volkwein A 2005 *Proceedings of Computing in Civil Engineering. ASCE, Cancun*
[2] Corominas J and Moya J 2008 *Engineering Geology* **102** 193–213 ISSN 00137952
[3] Peila D and Ronco C 2009 *Natural Hazards and Earth System Sciences* **9** 1291–1298
[4] Volkwein A, Schellenberg K, Labiouse V, Agliardi F, Berger F, Bourrier F, Dorren L K, Gerber W and Jaboyedoff M 2011 *Natural Hazards and Earth System Sciences* **11** 2617–2651
[5] Scavia C, Barbero M, Castelli M, Marchelli M, Peila D, Torsello G and Vallero G 2020 *Geosciences (Switzerland)* **10** 1–29

[6] Castanon-Jano L, Blanco-Fernandez E, Castro-Fresno D and Ballester-Muñoz F 2017 *Rock Mechanics and Rock Engineering* **50** 603–619
[7] Marchelli M 2020 *GEAM Geoingegneria Ambientale e Mineraria* **160** 24–35
[8] UNI 11211-4 2018 Opere di difesa dalla caduta massi - parte 4: Progetto definitivo ed esecutivo
[9] ONR 24810 2017 Technical protection against rockfall - terms and definitions, effects of actions, design, monitoring and maintenance
[10] Thompson P and Bellevue W 2015 Guidelines for certification and management of rockfall fence systems Tech. rep. Transportation Research Board
[11] Kalay Y E 1999 *Automation in construction* **8** 395–409
[12] Gottardi G and Govoni L 2010 *Rock mechanics and rock engineering* **43** 261–274
[13] Govoni L, de Miranda S, Gentilini C, Gottardi G and Ubertini F 2011 *International Journal of Physical Modelling in Geotechnics* **11** 126–137
[14] Mentani A, Giacomini A, Buzzi O, Govoni L, Gottardi G and Fityus S 2016 *Rock Mechanics and Rock Engineering* **49** 1247–1262
[15] Luciani A, Peila D and Barbero M 2016 *GEAM Geoingegneria Ambientale e Mineraria* **147** 31–38
[16] Coulibaly J B, Chanut M A, Lambert S and Nicot F 2019 *Rock Mechanics and Rock Engineering* **52** 4475–4496
[17] Qi X, Yu Z X, Zhao L, Xu H and Zhao S C 2018 *Advanced Steel Construction* **14** 479–495 ISSN 1816112X
[18] Koo R C, Kwan J S, Lam C and et al 2017 *Landslides* **14** 905–916
[19] EAD 340059-00-0106 2018 Falling rock protection kits
[20] Melchers R E and Beck A T 2018 *Structural reliability analysis and prediction* (John Wiley & Sons)
[21] EN 1997-1:2004 2004 Eurocode 7 - geotechnical design. part 1: General rules
[22] De Biagi V, Marchelli M and Peila D 2020 *Engineering Structures* **213** 110553
[23] Marchelli M, De Biagi V and Peila D 2020 *Geosciences* **10** 280
[24] Marchelli M, De Biagi V and Peila D 2021 *International Journal of Rock Mechanics and Mining Sciences* **139** 104664
[25] Piteau D and Clayton R 1976 Computer rockfall model *Proceedings of the meeting on rockfall dynamics and protective works effectiveness, Bergamo, Italy, ISMES Publication* vol 90 pp 123–125
[26] Piteau D and Clayton R 1976 *DR Piteau and Associates*
[27] Evans S and Hungr O 1993 *Canadian geotechnical journal* **30** 620–636
[28] Dorren L K 2003 *Progress in Physical Geography* **27** 69–87
[29] De Biagi V, Napoli M L and Barbero M 2017 *Natural hazards* **88** 1059–1086
[30] Vagnon F, Bonetto S, Ferrero A M, Harrison J P and Umili G 2020 *Geosciences* **10** 305
[31] Alejano L, Pons B, Bastante F, Alonso E and Stockhausen H 2007 *International Journal of Rock Mechanics and Mining Sciences* **44** 903–921
[32] Gili J, Ruiz-Carulla R, Matas G and et al 2016 *Landslides and engineered slopes: experience, theory and practice*
[33] Ruiz-Carulla R, Corominas J, Gili J A, Matas G, Lantada N, Moya J, Prades A, Núñez-Andrés M A, Buill F and Puig C 2020 *Geosciences* **10** 308
[34] Volta F 2011 *Il ruolo delle barriere paramassi nella mitigazione del rischio da frana nella provincia autonoma di Bolzano* Master's thesis Università di Bologna
[35] Ritchie A M 1963 Evaluation of rockfall and its control Tech. Rep. 17 Highway research record
[36] Pierson L A, Davis S A, Pfeiffer T J *et al.* 1994 The nature of rockfall as the basis for a new fallout area design criteria for 0.25: 1 slopes. Tech. rep. Dept of Transp, Oregon
[37] Nishimura T, Kiyama H, Fukuda T *et al.* 2008 Parametric three-dimensional simulations of dispersion of rockfall trajectories *The 42nd US Rock Mechanics Symposium (USRMS)* (American Rock Mechanics Association)
[38] Fischer L, Purves R S, Huggel C, Noetzli J and Haeberli W 2012 *Natural Hazards and Earth System Science* **12** 241–254
[39] Wang I T and Lee C Y 2010 *World Acad Sci Eng Technol* **65** 1021–1027
[40] Basharat M, Kashif M and Sarfraz Y 2018 *Quarterly Journal of Engineering Geology and Hydrogeology* **51** 387–398
[41] Pfeiffer T J and Bowen T 1989 *Bulletin of the Association of Engineering Geologists* **26** 135–146
[42] Azzoni A, La Barbera G and Zaninetti A 1995 *International journal of rock mechanics and mining sciences & geomechanics abstracts* **32** 709–724
[43] RocScience Inc 1998–2002 Rocfall, user's guide